Effect of Heat Input on the Mechanical and Metallurgical Characteristics of TIG Welded Joints

Subhas Chandra Moi[1], Pradip Kumar Pal[1], Asish Bandyopadhyay[1], Ramesh Rudrapati[2]*
[1]Mechanical Engineering Department,
Faculty of Engineering & Technology,
Jadavpur University, Kolkata-700032, India
[2]Mechanical Engineering Department,
Hawassa University-Institute of Technology, Hawassa - Ethiopia
**sc_moi1@rediffmail.com*

ABSTRACT

This paper presents the study of effect of heat input on the joint quality of tungsten inert gas (TIG) welded specimens. Three different heat input combinations selected as low heat (0.75kJ/mm), medium heat (0.90kJ/mm) and high heat (1.05kJ/mm) have been applied during the operation of TIG welding process on 316L austenitic stainless steel. Welded joints being prepared using a semiautomatic TIG welding machine, the effect of heat input is investigated on the weld bead geometry and mechanical-metallurgical characteristics of the joints. It is observed that as heat input increases, the width of weld bead increases, where as height of weld bead decreases with increasing heat input. Tensile strength as well as hardness increases with increase of heat input up to a threshold value and thereafter it start decreasing. The results of the investigation indicate that the joint prepared using medium heat input depicts higher tensile strength, percentage elongation, yield strength and higher micro hardness value than those joints made using low and high heat input due to smaller dendrite size and lesser interdendritic spacing in the weld zone and formation of very fine skeletal δ-ferrite in plain austenitic matrix. A large number of very fine and shallow dimples are observed in SEM fractograph of the joint made using medium heat input.

Keywords: *Tungsten Inert Gas Welding, Heat Input, Weld Bead Geometry, Microstructure, Tensile Strength.*

ISSN 1823-5514, eISSN2550-164X

Received for review: 2018-10-03
Accepted for publication: 2019-03-19
Published: 2019-08-31

Introduction

The stainless steel 316L is one of the most important materials for industrial uses because of its natural qualities. It is a non-magnetic material, cheaper in cost and easily available in the market. It possesses good mechanical properties like formability, ductility and weldability, toughness and high tensile strength at elevated temperature compare to other stainless steels [1]. 316L stainless steel belongs to 300 series grade of austenitic stainless steels. Here 'L' denotes an extra-low carbon version of austenitic stainless steel. This extra low carbon diminishes harmful carbide precipitation during welding. Austenitic stainless steels are extensively used for different applications which are as follows: pressure vessels, tanks, heat exchangers, piping systems, flanges, fittings, valves, pump trim, furnace parts, pharmaceutical industry, Surgical and medical tools, petroleum refining equipment, nuclear power plant, textile processing equipments etc. This stainless steel is usually found to be the most weldable due to its physical properties and welding activities compare to the other stainless steels. TIG welding is extensively used for joining of austenitic stainless steel materials.

Welding heat input is one of the most important key factors for controlling the heat and mass transfer, liquid flow and the thermo chemical responses that take place in molten weld pool. It is also an extremely significant factor to modify the chemistry of weld metal on solidification [2]. Kumar and Shahi [3] studied the impact of varying heat input on the mechanical and metallurgical properties of TIG welded AISI 304 stainless steel joints and concluded that as welding heat input increased, ultimate tensile strength as well as micro hardness value of weld metal and HAZ also decreased. Chuaiphan and Srijaroenpramong [4] reported the effect of different welding speed on mechanical properties and corrosion behaviour of welded AISI201 stainless steel. It is concluded that as welding speed increased weld face width and root width decreased and the pitting corrosion potential of weld metal increased due to small dendrite sizes and lesser inter dendritic spacing in the weld zone. Asif et. al. [5] investigated the influence of different heat input on mechanical properties, microstructure and corrosion of friction welded duplex stainless steel and found that as heat input increased, the micro hardness value also increased due to refinement of grains but tensile strength and impact toughness was found to be decreasing with an increase in heat input. An experimental investigation done by Durgutlu [6] on the effect of hydrogen in argon as a shielding gas in TIG welding of austenitic stainless steel and found that with increasing hydrogen content in shielding gas, grain size in the weld metal increased and at the same time the depth of penetration of the weld metal and weld bead width also increased. Mortazavi et. al. [7] studied the effect of three different heat inputs on microstructure and mechanical properties of dissimilar joints of

AISI 316L stainless steel and API X70 high-strength low-alloy steel. It is concluded that the dendrite size and interdendritic spacing in the weld metal is increased due to increase in heat input. As a result tensile strength and hardness are decreased but impact toughness is increased with increasing of heat input. Sadeghian et. al. [8] reported the impact of heat input on microstructure and mechanical characteristics of welded joints made by two dissimilar metals i.e. super duplex stainless steel and high strength low alloy steel. They concluded that as heat input increased the percentage of ferrite in the weld zone decreased. Again the joint made using high heat input depicted higher impact strength than the base those joints made using low heat input and base metal.

From literature study it is noticed that many investigators have been focused on various aspects of welded joints including microstructures, mechanical properties and corrosion resistance of stainless steel. But the investigation done by them is limited in so far as effect of heat input on the weld bead geometry and mechanical-metallurgical characteristics of TIG welded 316L austenitic stainless steel joints is concerned. In the present study, the effect of various heat input combinations on the weld bead geometry, microstructure, tensile strength, percentage elongation and micro hardness of AISI 316L stainless steel in a butt joint configuration has been investigated.

Experimental Procedures

Stainless steel (AISI 316L) plates of sizes 100 mm x 50 mm x 3 mm have been selected as work piece material which is cut from a rolled sheet and ER316L austenitic stainless steel of diameter 1.6 mm has been taken as a filler material. The chemical composition of the base metal (BM) and filler metal is shown in Table 1. The mechanical properties of the base metal are as follows: ultimate tensile strength 609MPa, yield strength 307MPa, modulus of elasticity 180GPa and hardness 202HV. The pictorial view of the experimental unit is shown in Figure 1. Here, the TIG torch has been fixed to the travel car to confirm the torch is set at a predetermined angle. The travel car travels on the defined path and can move only straight line direction. Control of current, speed and gas flow rate are done by manually for each run. All plates and filler rods are cleaned by stainless steel wire brush with acetone for removing the dust, oil, grease and thin oxide coating before welding. As plate thickness is 3 mm, no edge preparation or grooving is required. So, square butt joint configurations in flat position have been prepared by SUPERGEN 320 TIG welding machine using argon with purity 99.99%, as shielding gas. The welding direction has been taken as normal to the direction of rolling. To avoid distortion the work pieces have been placed

on copper plate and mechanical clamps are also used during welding. Various heat input combinations i.e. 0.75kJ/mm (low heat input), 0.90kJ/mm (medium heat input) and 1.05kJ/mm (high heat input) have been taken for the investigation. A huge number of trial experiments have been performed to identify these heat input combinations and these heat inputs are sufficient to cause full penetration welds. To find out the effects of heat input on the microstructure and mechanical properties of TIG welded joints an increasing step of 25A current has been taken. Chemical composition of weld metal (WM) is also examined and obtained result is shown in Table 1. Table 2 represents the different welding parameters which are used during welding.

Table 1: Chemical composition (wt.%) of the BM, filler metal & WM

Alloy element	C	Mn	Si	S	P	Cr	Ni	Mo	Fe
AISI316L	0.026	0.97	0.26	0.012	0.043	16.12	10.08	2.03	Bal.
ER316L	0.040	1.50	0.45	0.030	0.030	18.20	12.00	2.30	Bal.
Weld Metal	0.031	1.41	0.33	0.021	0.034	17.23	10.88	2.23	Bal.

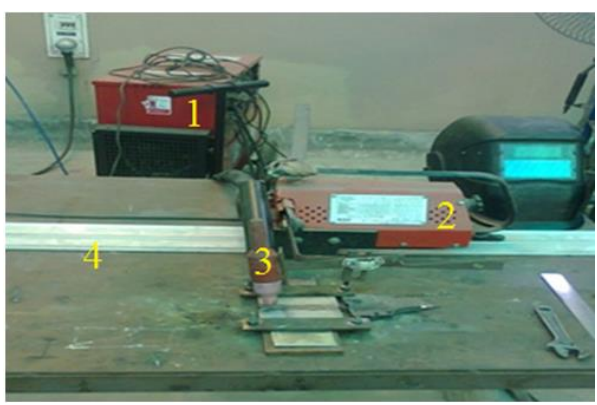

1-welding machine
2-travel car
3-TIG torch
4- track

Figure 1: Photographic view of experimental setup

After welding all the joints have been inspected visually and no significant defects has been observed in any of the specimens. Then other destructive and non-destructive tests have also been conducted like X-ray radiography test, tensile test etc. In each condition of heat input, three specimens have been conducted for different tests and the average result has been tabulated here. It is found that almost all the specimens pass through X-ray radiography test with no significant defect remarks. The welded specimens have been made ready for the metallographic examinations by

polishing and etching, to determine the chemical, atomic structure and spatial distribution of all types of constituents, phases in the welded specimen. Micro-hardness test has also been done using Vickers's micro-hardness testing machine on flat metallographic specimen across the joints. The tensile test specimens have been prepared according to ASTM E8M-04 as shown in Figure 2. Tensile test has been performed by Instron universal testing machine (Model-8801) at a strain rate of 0.001/s. Furthermore, the fractured surfaces are analyzed by SEM fractrography.

Table 2: TIG welding process parameters

Specimen no.	Current (A)	Welding speed (mm/min)	Voltage (V)	Gas flow rate (l/min)	Heat input (kJ/mm)
1	100	120	25	9	0.75 (low heat)
2	125	150	30	9	0.90 (medium heat)
3	150	180	35	9	1.05 (high Heat)

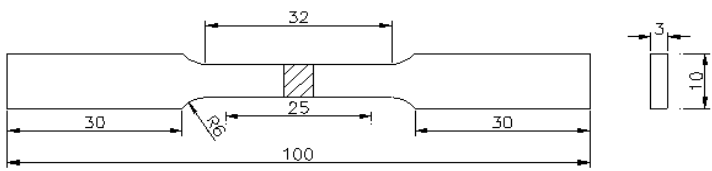

Figure 2: TIG welded specimen for tensile test

Results and discussion

Metallographic studies

All the welded joints have been prepared for the measurement of weld bead geometry and micro structural investigation (including base metal) according to standard procedure using toolmaker's microscope and scanning electron microscope (SEM) respectively. Table 3 represents macro and microstructure details of welded joints. Typical SEM micrograph of the base metal is shown in Figure 3. Figures 4-6 illustrate the SEM micrographs of HAZ - fusion boundarty (FB) - weld metal (WM) and weld zone of 3 difiierent specimens for different heat input combinations. It is noticed that width of weld bead increases with increase of heat input, where as height of weld bead decreases

with increase of heat input. It is also observed from SEM micrographs that dendrite size and inter-dentritic spacing decreases with increase of heat input there after it starts increasing.

Table 3: Macro and microstructure particulars of welded joints

Specimen no.	Macrostructure details		Microstructure details	
	Weld width (mm)	Weld Height (mm)	Dendrite length (μm)	Interdendritic spacing (μm)
1. (low heat)	6.01	1.32	131.21	14.14
2. (Medium heat)	6.15	1.28	95.54	10.12
3. (high heat)	6.56	1.25	168.25	18.22

The microstructure of base metal is completely different from weld metals irrespective of heat input. Fully austenitic structure with little annealing twins is observed in base microstructure. Wichan and Loeshpahn [9] are also reported similar result. The microstructure of these weld metals consists of ferrite and austenite i.e. δ-ferrite structure that could be described by primary solidification modes of weld metals. The weld metal solidification mode can be explained by the Cr_{eq}/Ni_{eq} ratio. The Cr_{eq}/Ni_{eq} ratio is calculated using the Schaeffler formula [10]. In the present study the Cr_{eq}/Ni_{eq} = 1.59. Therefore the solidification mode is ferritic-austenitic mode (FA) as $1.48 \leq Cr_{eq}/Ni_{eq} \leq 1.95$.

FA mode: $L \rightarrow L+\delta \rightarrow L + \delta + \gamma \rightarrow \delta + \gamma \rightarrow \gamma : 1.48 \leq Cr_{eq}/Ni_{eq} \leq 1.95$

where L is the liquid, δ is delta-ferrite and γ is austenite respectively.

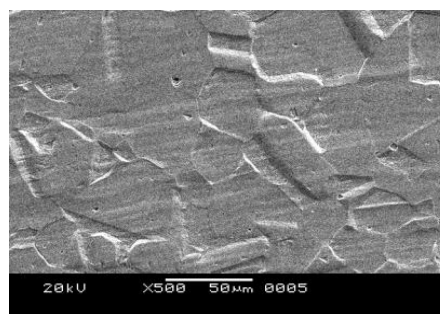

Figure 3: Microstructure of base metal

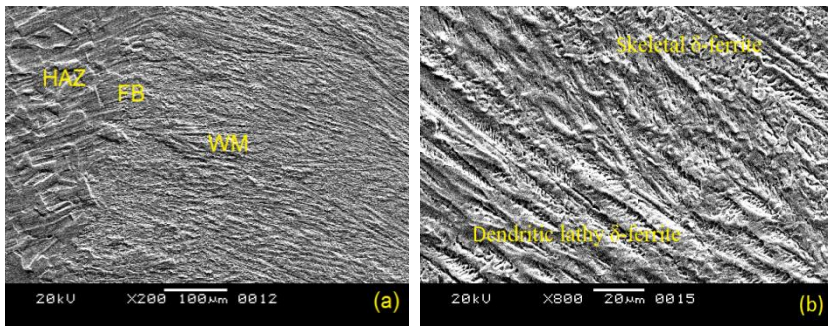

Figure 4: SEM micrographs of (a) HAZ and fusion boundary (b) weld zone (low heat input)

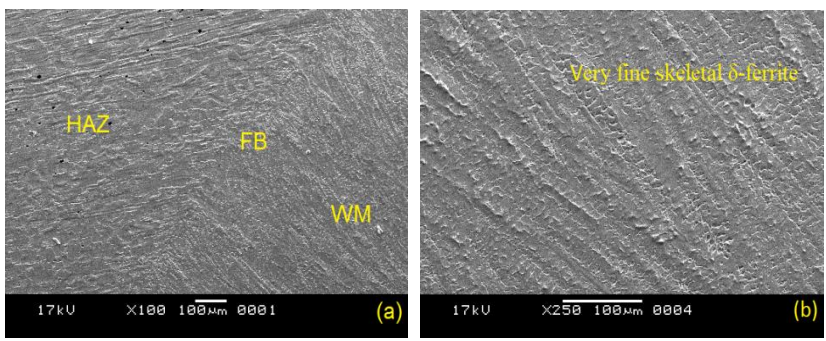

Figure 5: SEM micrographs (a) HAZ and fusion boundary (b) weld zone (medium heat input)

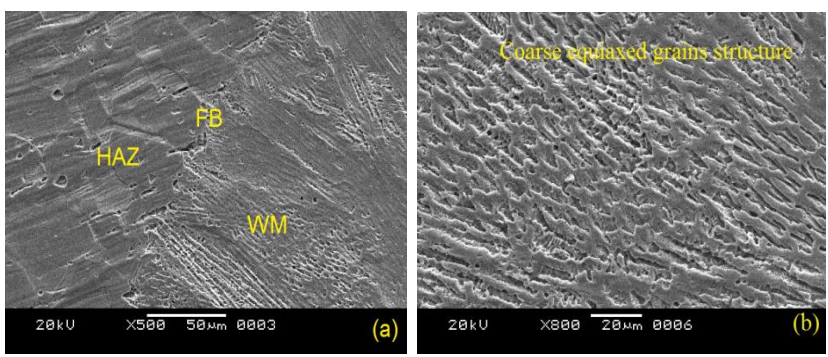

Figure 6: SEM micrographs of (a) HAZ and fusion boundary (b) weld zone (high heat input)

The weld specimen no.1 which is made with low heat input consists of skeletal δ-ferrite in plain austenitic matrix and δ-ferrite in the form of dendritic lathy δ-ferrite at the dendrite core surrounded by inter dendritic γ-phase due to high cooling rates – this is the result identified from the metallographic studies. Again, the weld zone of the specimen made with medium heat input exhibits a very fine skeletal δ-ferrite in plain austenitic matrix due to moderate cooling rate. The microstructure of the weld, specimen no. 3 (high heat input) depicts a coarse equiaxed grains structure which has been formed due to the decomposition of dendritic grains in plain austenitic matrix and coarse HAZ zone is also formed.

Micro hardness

After micro structural analysis micro-hardness experiment has been performed by Vickers's micro-hardness testing machine on etched transverse cross section of the welded specimens using a load of 100g, which is applied for duration of 10s. The profile of micro-hardness for three different specimens is shown in Figure 7. It is noticed that all three welded joints show higher the micro-hardness value at weld zone/ fusion zone with respect to the base metal and HAZ zone. Similar result has been reported by Buddu et.al. and Kumar et.al. [11]-[12]. As the indenter passes through from fusion boundary to weld center the hardness value increases from 212 to 234HV for low heat input, 213 to 240HV for medium heat input and 211 to 227HV for high heat input welded joint. The specimen welded with low heat input depicts higher hardness value and specimen welded using high heat input shows lowest harness value in the weld zone due to lower δ-ferrite content and relatively coarse grain structure. The specimen made using medium heat input having highest hardness values due to higher δ-ferrite content and having relatively finer grain structure. The variation in hardness values in different weld specimens may be induced by their microstructure refinement due to the quick solidification of the weld pool.

Tensile Properties

The uniaxial tensile test of base metal along with all the welded specimens made using various heat input combinations has been carried out to essess the joint strength at room temperature. In each condition of heat input, three specimens have been conducted for tensile test and the average ultimate tensile strength (UTS) and their corresponding percentage elongations (% δl) and yield strength (σ_Y) are tabulated in Table 4. Again, stress-strain curve of three welded specimens is also shown in Figure 8. All the welded specimens are fractured at HAZ-base interface and the base metal is fractured at the centre of the gauge length. It is found that the maximum and minimum ultimate tensile strength of 645.45MPa and 620.21MPa are obtained by the welded joints made using medium heat input and high heat input

respectively. The tensile strength increases with the increase of heat input up to a threshold value and thereafter it stars decreasing. Similar pattern is found in case of percentage elongation, as well as yield strength also. The specimen no.2 exhibits 2.04% higher tensile strength compare to specimen no.1 and 4.07% more strength compare to specimen no.3. In case of percentage elongation is concerned, specimen no.2 depicts 17.57% and 8.07% more value compare to specimen no.1 and specimen no.3 respectively. Yield strength of the specimen made using medimum heat input is also increased significantly in compare to others. This is due to formation of very fine skeletal δ-ferrite grains in the weld region, moderate precipitation and smaller dendrite size and inter-dentritic spacing [13]. The reason of lowest tensile strength obtained by specimen no. 3 (high heat input) is formation of coarse equiaxed grains structure in the weld zone and higher dendrite size and inter-dentritic spacing. This is in line with the micro-hardness data. The base metal has lowest UTS (608.92), yield stress (306.92MPa) and percentage elongation compared to these three welded specimens.

Table 4: Tensile properties of base metal and welded joints

Specimen no.	Tensile properties			Joint efficiency (%)
	UTS (MPa)	% δl	σ_Y (MPa)	
1. (low heat)	632.56	44.4	374.45	103.88
2. (Medium heat)	645.45	52.2	385.32	105.99
3. (high heat)	620.21	48.3	369.21	101.85
Base Metal	608.92	42.4	306.98	---

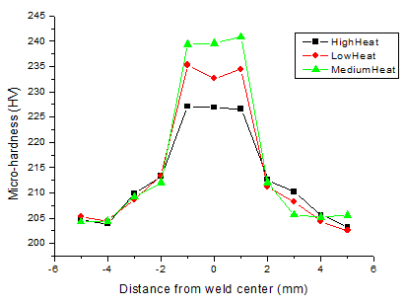

Figure 7: Micro-hardness profile

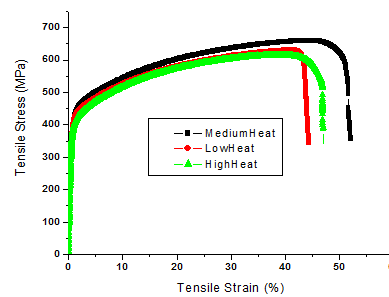

Figure 8: Stress-strain curve

The fracture surfaces obtained from tensile test of base metal and three welded specimens have been examined using scanning electron microscope and the obtained result is shown in Figure 9. Figure 9(a) represents high

magnification fracture morphology of base metal. The fracture surfaces consist of many equiaxed dimples of varying size and shape, micro voids and voids. There is no surface cracks are observed. These are the characteristics of ductile fracture. Figure 9(b)-(d) shows high magnification SEM fractograph of weld specimens prepared using different heat inputs. Significant disparity is observed in the surface morphology, like size of the dimples, surface cracks etc. between weld specimens made using low, medium and high heat input. It is may be due to different cooling rate for the different weldments. High heat input, results in slow cooling rate and it will take longer time for solidification. As a result it produces coarse grain, hence coarse dimples.

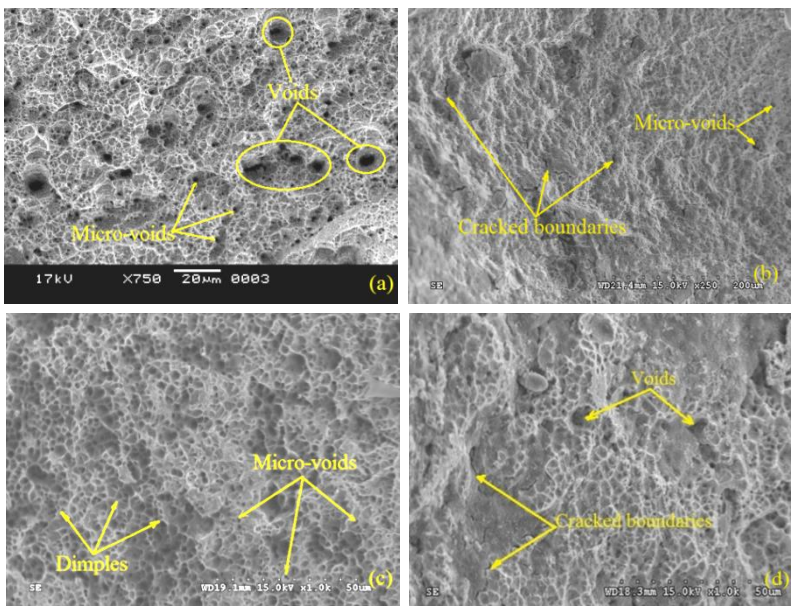

Figure 9: SEM fractograph of (a) base metal, weld specimens made using (b) low heat input (c) medium heat input (d) high heat input.

It is noticed from SEM fractographs that the specimen no.1 (low heat input) consist of fine dimples and voids. Some crack boundaries are also observed. In case of specimen no.2 (medium heat input), a large number of very fine and shallow dimples is observed and surface cracks are also invisible. This is in line with the metallographic results. The specimen 2 consists of a large number of very fine skeletal δ-ferrite in plain austenitic matrix. An increase in the δ-ferrite content leads to an increase in the strength [14]-[15]. In case of specimen no.2, a large number of very fine and shallow

dimples is observed and surface cracks are also invisible. This is the reason for its highest tensile strength and percentage elongation. Whereas, elongated dimples with voids is found in high heat inputted specimen [16]. Some cracks are also noticed here.

Conclusions

The effect of heat input on the mechanical-metallurgical characteristics of TIG welded 316L stainless steel joints is investigated and it is found that as heat input increases, the width of weld bead also increases, where as height of weld bead decreases with increase of heat input.

The micro hardness value of all the weld joints is found to be of remarkably higher as compare to those of HAZ zone and base metal irrespective of heat input combination. Micro hardness value as well as tensile strength increases with increase of heat input up to a certain limit and thereafter it start decreasing. The joint made using medium heat input depicts the considerable increase of tensile strength, percentage elongation and hardness due to finer grain structure, smaller dendrite size and inter-dentritic spacing as compared to low heat and high heat conditions.

A large number of very fine and shallow dimples are observed in SEM fractograph of the joint made using medium heat input, where elongated dimples with voids are found in the joint made using high heat input.

References

[1] N. Ghosh, P. K. Pal, G. Nandi, R. Rudrapati, "Parametric optimization of gas metal arc welding process by PCA based Taguchi method on austenitic stainless steel AISI 316L," Materials Today: Proceedings 5, pp 1620-1625, 2018.

[2] S. Junsheng and W. U. Chuansong, "The effect of welding heat input on the weldpool behavior in MIG welding," Science in China (Series E) 45 (3), pp 291-299, 2002.

[3] S. Kumar and A. S. Shahi, "Effect of heat input on the microstructure and mechanical properties of gas tungsten arc welded AISI 304 stainless steel joints," Materials and Design 32, pp 3617-3623, 2011.

[4] W. Chuaiphan and L. Srijaroenpramong, "Effect of welding speed on microstructures, mechanical properties and corrosion behavior of GTA-welded AISI 201 stainless steel sheets," Journal of Materials Processing Technology 214, pp 402-408, 2014.

[5] M. Asif M, K. A. Shrikrishna, P. Sathiya, S. Goel, "The impact of heat input on the strength, toughness, microhardness, microstructure and

corrosion aspects of friction welded duplex stainless steel joints," Journal of Manufacturing Processes 18, pp 92-106, 2015.

[6] D. Ahmet, "Experimental investigation of the effect of hydrogen in argon as a shielding gas on TIG welding of austenitic stainless steel," Materials and Design 25, pp 19-23, 2004.

[7] E. Mortazavi, R. A. Najafabadi, A. Meysami, "Effect of heat input on microstructure and mechanical properties of dissimilar joints of AISI 316L steel and API X70 high-strength low-alloy steel," Journal of Iron and Steel Research, International 24 (12), pp 1248-1253, 2017.

[8] M. Sadeghian, M. Shamanian, A. Shafyei, "Effect of heat input on microstructure and mechanical properties of dissimilar joints between super duplex stainless steel and high strength low alloy steel," Materials and Design 60, pp 678-684, 2014.

[9] C. Wichan and S. Loeshpahn, "Effect of filler alloy on microstructure, mechanical and corrosion behaviour of dissimilar weldment between AISI 201 stainless steel and low carbon steel sheets produced by a gas tungsten arc welding," Advanced Materials Research 581-582, pp 808-816, 2012.

[10] John C. Lippold and Damian J. Kotechi, "Welding metallurgy and weldability of stainless steels", (Wiley-Interscience), pp 29-31, 2005.

[11] R. K. Buddu, N. Chauhan, P. M. Raole, "Mechanical properties and microstructural investigations of TIGwelded 40 mm and 60 mm thick SS 316L samples for fusion reactorvacuum vessel applications," Fusion Engineering and Desig 89, pp 3149-3158, 2014.

[12] N. Kumar, M. Mukherjee, A. Bandyopadhyay, "Study on laser welding of austenitic stainless steel by varying incident angle of pulsed laser beam," Optics and Laser Technology 94, pp 296-309, 2017.

[13] G. Padmanaban and V. Balasubramanian, "optimization of laser beam welding process parameters to attain Maximum tensile strength in AZ31B magnesium alloy," Optics & Laser Technology 42, pp 1253-1260, 2010.

[14] A. Gigovi-Geki, M. Oru, S. Muhamedagi, "Effect of the delta-ferrite content on the tensile properties in nitronic 60 steel at room temperature and 750°C," Materials and technology 46 (5), pp 519–523, 2012.

[15] Y. Jun, G. Ming, Z. Xiaoyan, "Study on microstructure and mechanical properties of 304 stainless steel joints by TIG, laser and laser-TIG hybrid welding," Optics and Lasers in Engineering 48, pp 512–517, 2010.

[16] C. Muthusamy, L. Karuppiah, S. Paulraj, D. Kandasami, R. Kandhasamy, "Effect of Heat Input on Mechanical and Metallurgical Properties of Gas Tungsten Arc Welded Lean Super Martensitic Stainless Steel," Materials Research 19 (3), pp 572-579, 2016.